Original Article

Resolution Recovery with Pre-Reconstruction Fourier Transforms Filtering for a High Resolution Animal SPECT System

Reza Hashemi Shahraki [1], Isaac Shiri [2], Parham Geramifar [3], Afshin Akbarzadeh [2], Amir Hossein Sanaat [4], Mohammad Reza Ay [1,2,*]

[1] Department of Medical Physics and Biomedical Engineering, School of Medicine, Tehran University of Medical Sciences, Tehran, Iran

[2] Research Center for Molecular and Cellular Imaging, Tehran University of Medical Sciences, Tehran, Iran

[3] Research Center for Nuclear Medicine, Shariati Hospital, Tehran University of Medical Sciences, Tehran, Iran

[4] Faculty of Nuclear Engineering and Physics, Amirkabir University of Technology, Tehran, Iran

Received: 24 May 2018

Accepted: 03 November 2018

http://FBT.tums.ac.ir

Keywords:

Resolution Recovery;

Image Reconstruction;

Filter;

Animal Single Photon Emission Computed Tomography.

Abstract

Purpose: Spatial resolution and accurate quantification in animal SPECT plays a critical role in preclinical imaging. Appropriate Projections filtering can help to address the issue of resolution compensation and recovery coefficients. The main aim of current study was to explore a new version of MLEM algorithm with pre-reconstruction Fourier transform filtering to improve the Recovery Coefficient RC by filtering the projections.

Materials and Methods: A complete set of measurements was performed using HiReSPECT system. Different phantom studies were performed using point sources, NEMA NU 4 and dedicated hot rod phantom. All data was reconstructed using the developed Maximum-Likelihood Expectation-Maximization (MLEM) algorithm with and without resolution recovery information and also with our presented pre-reconstruction Fourier transform filter. Image quality was assessed by different parameters such as Coefficient Of Variation (COV), Recovery Coefficient (RC) and FWHM.

Results: FWHM in tangential direction was improved 0.6 and 0.2 for our presented algorithm against MLEM without and with CDRF, respectively. Fourier filtering image led to improvement of image quality where hot rods with 1.6 and 1.8 mm in diameter could be recognized clearly in our presented algorithm in dedicated hot rod phantom. Our presented algorithm resulted in rapid convergence and growth of RC in lower iteration.

Conclusion: The purpose of the current study was to introduce new pre-reconstruction filter. The results of this investigation showed that the inclusion of our proposed filter can lead to better image quality and quantification in lower iteration. These data suggest that current filter can provide higher RC in lower iteration.

1. Introduction

Preclinical imaging with Single Photon Emission Computed Tomography (SPECT) plays a key role in translational researches. Spatial resolution and accurate quantification in animal SPECT plays a critical role in capturing of molecular events in living small animal [1]. Accurate activity quantification in SPECT leads to improvement in targeted radio-immunotherapy and precise molecular imaging researches [2-7].

Major issues in accurate quantification of activity include statistical noise, photon attenuation, photon

Corresponding Author:
Mohammad Reza Ay, PhD
Department of Medical Physics and Biomedical Engineering, School of Medicine, Tehran University of Medical Sciences, Tehran, Iran
Tel: (+98)21 66907518
Email: mohammadreza_ay@tums.ac.ir

scatter, collimator-detector response and patient motions [4, 8-10]. A considerable amount of literature has been published to improve the quantitative accuracy in SPECT by using various correction methods such as attenuation correction, Collimator-Detector Response Function molding (CDRF) in image reconstruction and resolution recovery. Collimator-detector response is the main image blurring factor in SPECT, and there are several methods have been proposed to correct in sinogram (both spatial and Fourier space).[2, 4, 7, 11, 12].

Sinogram correction can be done with convolution or high pass filters [16]. Different kinds of filters have been previously used in SPECT imaging to improve quantification and noise reduction [13, 14]. Recent evidence suggests that restoration filter after Fourier transformation of the sinogram can be an alternative approach for compensation of resolution [6, 12, 15].

Projections filtering by using appropriate filter can play an important role in addressing the issue of resolution compensation and recovery coefficients. The main aim of current study is to explore a new version of MLEM algorithm which improves the Recovery Coefficient (RC) by pre-reconstruction Fourier transform filtering [15-17].

2. Materials and Methods

2.1. Animal SPECT Scanner (HiReSPECT)

A complete set of measurements was performed using HiReSPECT system. HIRespect is a dual head preclinical SPECT and each head of scanner consists of pixelated scintillator crystal tightly attached to two position sensitive PMTs (PSPMT). High resolution parallel-hole collimator with an active collimating area of 108×56 mm^2 was used to eliminate scatter photons. Scanner spatial resolution is 1.7 and 1.6 mm in planar and tomographic mode, respectively, and system sensitivity is about 1.3 cps/µCi [1, 18].

2.2. Phantom

2.2.1. Point Source

Three ^{99m}Tc point sources with inner diameter of 1.1 mm and 0.5 µCi activity were placed in the Field Of View (FOV); one at center and two displaced 10 mm from axis of rotation. Data acquisition for point source was performed by 60 seconds for each projection (60 views over 360 degrees).

2.2.2. NEMA NU-4 IQ Phantom

The NEMA- NU 4 IQ phantom (Figure 1.) is composed of a fillable cylindrical chamber with 30 mm in diameter and length which consists of 3 main parts [19-21]. The first part contains 5 fillable rods in different diameters (1, 2, 3, 4 and 5 mm), which were used to determine spatial resolution and activity recovery coefficients. The Second part is a hollow cylinder, which was filled with uniform activity to measure Coefficient Of Variation (COV). The Third part consists of two hollow cylinders, 15 mm in length and 8 mm in inner diameter, which are indicative of the spillover and scatter correction performed by activity measurement in two compartments. The phantom was filled with uniform solution of normal saline and 5mCi of Tc-99m, and subsequently data acquisition was performed 120 seconds for each projection (60 views over 360 degrees).

Figure 1. NEMA NU-4 IQ phantom used to assess the reconstructed image quality of the system

2.2.3. Dedicated Hot Rod Phantom

Dedicated hot rod phantom (Figure 2) is 'Jaszczak-like' phantom which is composed of a fillable cylindrical chamber with 35 mm in diameter and 32 mm in length and contains six sections of hot rods in diameters of 1.6, 1.8, 2, 2.2, 2.4, and 2.6 mm [18]. For data acquisition, hot rod phantom was filled with homogenous solution of normal saline and 2 mCi ^{99m}Tc,

and each projection was acquired with 60 seconds (60 views over 360 degrees).

Figure 2. The dedicated in house hot rod phantom designed for tomographic spatial resolution characterization

2.3. Image Reconstruction

All data was reconstructed using the developed Maximum-Likelihood Expectation-Maximization (MLEM) algorithm with and without resolution recovery information and also with our presented filter (with 1, 2, 3, 4, 5, 10, and 15 iterations).

The developed MLEM algorithm uses FBP algorithm to produce first approximation of initial image. The MLEM algorithm produces image through following Equation 1:

$$f_j^{(n+1)} = \frac{f_j^{(n)}}{\sum_i H_{ij}} \sum_i H_{ij} \frac{P_i}{\sum_k H_{ik} f_k^{(n)}} \qquad (1)$$

Where $f_j^{(n)}$ is the current voxel value of j, and $f_j^{(n+1)}$ is the next estimation of voxel j based on pervious estimation. In this algorithm, images produced by FBP were used to first guess ($f^{(0)}$), for initialization of reconstruction image. To produce first guess image we used our developed ramp like filter (against ramp filter in conventional reconstruction) by the following Equation 2:

$$H(f) = \begin{cases} 0.15, & 0 \le f < 0.007 \\ 0.1, & 0.007 \le f < 0.056 \\ f + 0.1, & 0.056 \le f < 0.5 \\ 0.1, & f \ge 0.5 \end{cases} \qquad (2)$$

Following first guess image, next projections were filtered by the following filter: Figures 3 and 4 show these filters.

$$H'(f) = \begin{cases} 0.05, & 0 \le f < 0.056 \\ f + 0.05, & 0.056 \le f < 0.5 \\ 0.05, & f \ge 0.5 \end{cases} \qquad (3)$$

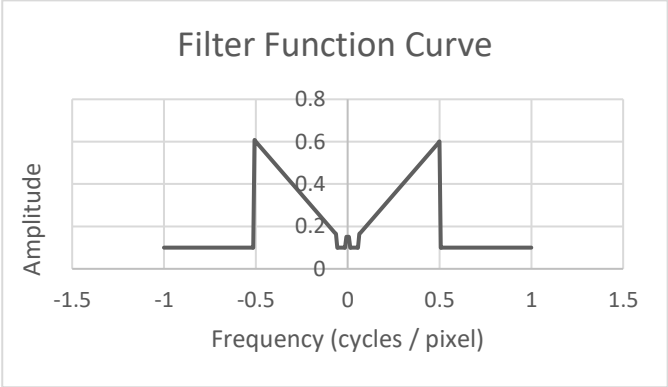

Figure 3. Filter curve used in FBP reconstruction

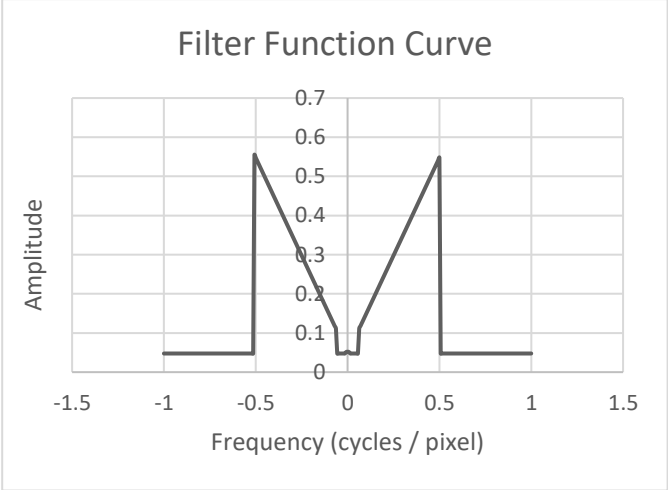

Figure 4. Filter curve used in our presented algorithm

2.4. Analysis of Results

Quality of images was assessed by different parameters such as Coefficient Of Variation (COV), Recovery Coefficient (RC) and FWHM. Spatial resolution was measured in terms of FWHM along the tangential, radial and central direction. RC is expressed as the measured activity concentration in the rods divided by the mean phantom activity [22]. The COV was used to quantify image noise in uniform phantom background.

3. Results

3.1. Spatial Resolution

Table 1 provides the results obtained from the preliminary analysis of tomographic spatial resolution analysis from capillary source in tangential, radial and central direction. It is apparent from this table that FWHM in tangential direction is improved 0.6 and 0.2 for our presented algorithm against MLEM without and with RR, respectively.

Table 1. Tangential, radial, and central spatial resolution (FWHM in mm) for different image reconstruction methods

View	MLEM with Fourier filtering	MLEM with RR	MLEM without RR
Tangential(mm)	1.4	1.7	3.2
Radial(mm)	1.5	1.7	3.2
Central(mm)	1.5	1.8	3.3

Figure 5. presents trans-axial image of dedicated hot rod phantom for MLEM with and without RR and also with our presented algorithm (at the same number of iteration). It can be observed that Fourier filtering can lead to improvement of image quality. From Figure 5 the hot rods in section 1.6 and 1.8 could be clearly recognized in our presented algorithm.

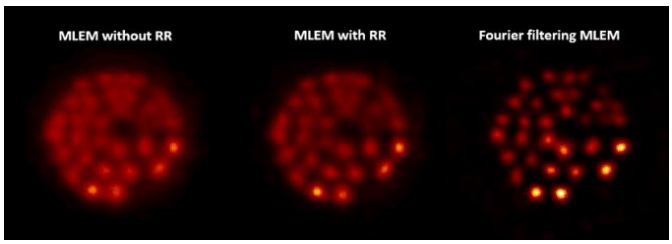

Figure 5. Transverse view of dedicated in house hot rod phantom. Images of the phantom were reconstructed with different algorithms (left) MLEM without RR (middle) MLEM with RR (right) Fourier filtering MLEM

3.2. Recovery Coefficients

Quantitative analysis in Figures 6-9 shows RC as a function of iteration in different sphere size of NU 4IQ phantom. The Figures 7-10 show that there has been a gradual rise in the RC for our presented algorithm from iteration 5. At the same time, the amount of RC for other reconstruction remains steady. What stands out in the graphs is the continual growth of RC in all RODs but the amount of RC is likely to be high in bigger RODs.

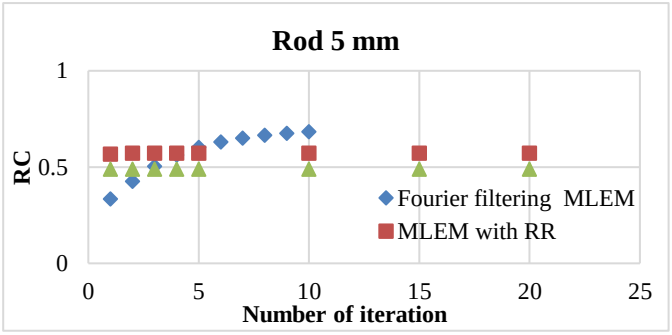

Figure 6. RCs of 5 mm rod for various iterations

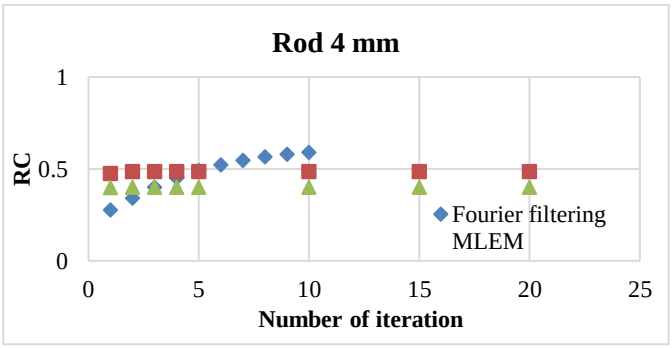

Figure 7. RCs of 4 mm rod for various iterations

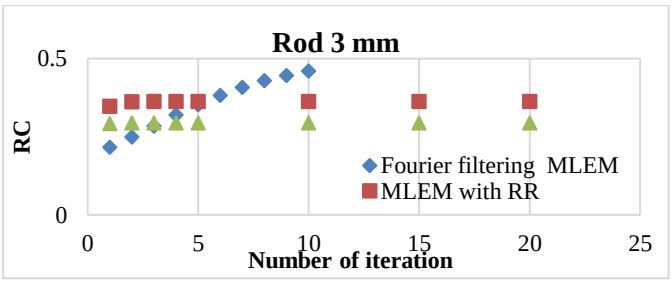

Figure 8. RCs of 3 mm rod for various iterations

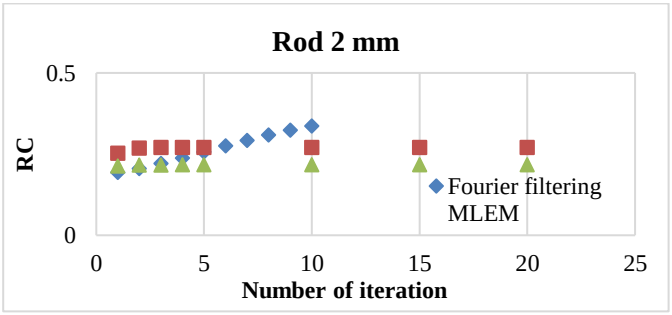

Figure 9. RCs of 2 mm rod for various iterations

What can be clearly seen in graphs is the rapid convergence and growth of RC in our presented algorithm in lower iteration (1-5 iterations). Figure 10. reveals that there has been a continued improvement in

image quality by increasing iteration in our presented algorithm.

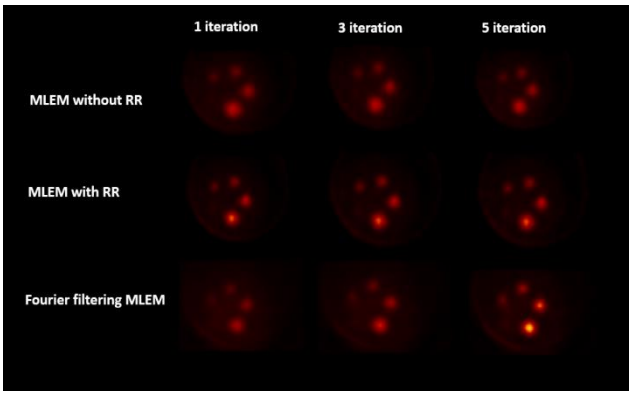

Figure 10. Transverse view of NU 4 IQ phantom. Images of the phantom for different algorithms were shown for 1, 3 and 5 iteration

3.3. Noise

Figure 11. shows coefficient of variation in uniform region of IQ 4 U phantom as a function of iteration in different reconstruction algorithms. The proposed algorithm reached the same noise level from 1-5 iteration, but it leads to a phenomenal growth in coefficient of variation.

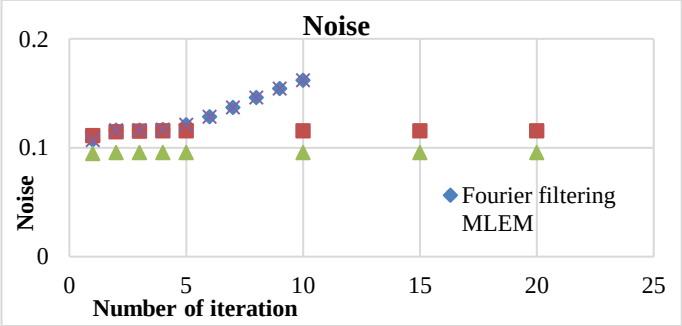

Figure 11. Noise in Uniform Phantom Region as function of number of iterations

4. Discussion

Image quality in SPECT depends on several factors such as statistical noise, photon attenuation, photon scatter, collimator-detector response and image reconstruction algorithm [1-3, 12, 23]. The main challenge that many researchers are faced with is small organ imaging in preclinical researches and one of the key factors to determine SPECT performance is the resolution of system [24].

A number of cross-sectional studies suggested different methods such as inclusion of compensation of distance dependent resolution recovery (which is called CDFR molding) and pre-reconstruction filtering to improve SPECT image resolution [1-3]. For collimator-detector response correction in SPECT. Xia *et al.* used projection filtering. They improved resolution of reconstructed image. Prior studies have noted the importance of filters in reconstruction process to improve resolution [6, 13, 17, 25]. This study set out to assess the performance of new version of MLEM algorithm which uses projection filtering process. For, algorithm validation we used simulation data in MATLAB. For this purpose, we produce different projection of Shepp-Logan phantom, then, the reconstructed images were compared by Normalized Square Error (NSE) with ground truth phantom images [25-27].

Ramp filter is a high pass filter and decline low frequencies, which leads to image blurring and elimination of star artifact [13]. Amplification of statistical noise and detrition of resolution in iterative reconstruction is one of the most frequently stated problems in preprocessing of projection with ramp filter. This study seeks to modify ramp filter which will help to address these issues.

A key aspect of the current filter is to permit very low and high frequencies. A previous research has established that CDRF modeling in HiReSPECT resulted in 1.7 mm tomographic spatial resolution, whereas the spatial resolution in presented algorithm reaches 1.5 mm.

The results of this study indicate that the value of RC is likely to be low in small RODs, thus small RODs need more iterations to reach higher RC. One interesting finding in current study is increasing RC with rapid convergence in lower iterations in our presented algorithm. However, the current study leads to increase noise in higher iterations. For quantitative comparison of resolution improvement, we reconstructed image of point source by 3 algorithms, then we calculated FWHM in different axis.

Previous studies and current study show that high pass filter in frequency space of sinogram leads to noisier image. Comparison of the findings with other studies confirms that the resolution recovery method increases the noise level. Recent work done by Zeratkar *et al.* [1] has established that CDRF modeling leads to increase RCs and simultaneously noise level. In presented algorithm the increased number of iteration leads to higher RCs as well as higher noise level. The increment of RCs and noise are higher than CDRF modeling, however the overall level of RC was found to be 3-6% higher than that of previously reported levels. This result may be explained by the fact that current algorithm passes some high frequencies, which leads to increase statistical noise. The limitations of this work are mainly in the limited number of subjects included in this study and also phantom not containing all range of data frequency used in preclinical studies. The results of this study could be confirmed in a rat and mice dataset.

5. Conclusion

The purpose of the current study was to introduce a new pre-reconstruction filter. The results of this investigation showed that the inclusion of our proposed filter can result in better image quality and quantification in lower iteration. These data suggest that the current filter can provide higher RC in lower iteration. One of the limitations of current algorithm is the increase in noise in higher iteration. However, in spite of this limitation, the algorithm favorably leads to higher convergence in lower iterations.

References

1- N. Zeraatkar *et al.*, "Resolution-recovery-embedded image reconstruction for a high-resolution animal SPECT system," *Physica Medica*, vol. 30, no. 7, pp. 774-781, 2014.

2- S. Y. Chun, J. A. Fessler, and Y. K. Dewaraja, "Correction for collimator-detector response in SPECT using point spread function template," *IEEE transactions on medical imaging*, vol. 32, no. 2, pp. 295-305, 2013.

3- S. Y. Chun, J. A. Fessler, and Y. K. Dewaraja, "Post-reconstruction non-local means filtering methods using CT side information for quantitative SPECT," *Physics in medicine and biology*, vol. 58, no. 17, p. 6225, 2013.

4- S. J. Glick, B. C. Penney, and M. A. King, "Filtering of SPECT reconstructions made using Bellini's attenuation correction method: a comparison of three pre-reconstruction filters and a post-reconstruction Wiener filter," *IEEE transactions on nuclear science*, vol. 38, no. 2, pp. 663-669, 1991.

5- K. Murase, S. Tanada, Y. Yasuhara, H. Mogami, A. Iio, and K. Hamamoto, "SPECT volume measurement using an automatic threshold selection method combined with a V filter," *European journal of nuclear medicine*, vol. 15, no. 1, pp. 21-25, 1989.

6- J. H. Kim and K. I. Kim, "A count-dependent reconstruction filter optimized to match the lesion size and the object contrast in SPECT," *IEEE transactions on nuclear science*, vol. 42, no. 4, pp. 1321-1330, 1995.

7- T. Yokei, H. Shinohara, and H. Onishi, "Performance evaluation of OSEM reconstruction algorithm incorporating three-dimensional distance-dependent resolution compensation for brain SPECT: a simulation study," *Annals of Nuclear Medicine*, vol. 16, no. 1, pp. 11-18, 2002.

8- P. Ritt, H. Vija, J. Hornegger, and T. Kuwert, "Absolute quantification in SPECT," *European journal of nuclear medicine and molecular imaging*, vol. 38, no. 1, pp. 69-77, 2011.

9- W. Römer *et al.*, "Attenuation correction of SPECT images based on separately performed CT," *Nuklearmedizin*, vol. 44, pp. 20-8, 2005.

10- R. M. Lewitt, P. R. Edholm, and W. Xia, "Fourier method for correction of depth-dependent collimator blurring," in *Medical Imaging III: Image Processing*, 1989, vol. 1092, pp. 232-244: International Society for Optics and Photonics.

11- E. O'Mahoney and I. Murray, "Evaluation of a matched filter resolution recovery reconstruction algorithm for SPECT-CT imaging," *Nuclear medicine communications*, vol. 34, no. 3, pp. 240-248, 2013.

12- H. Mahani, G. Raisali, A. Kamali-Asl, and M. R. Ay, "Collimator-detector response compensation in molecular SPECT reconstruction using STIR framework," *Iranian Journal of Nuclear Medicine*, vol. 25, pp. 26-34, 2017.

13- M. Lyra, A. Ploussi, M. Rouchota, and S. Synefia, "Filters in 2D and 3D cardiac SPECT image processing," *Cardiology research and practice*, vol. 2014, 2014.

14- A. Seret and J. Forthomme, "Comparison of different types of commercial filtered backprojection and ordered-subset expectation maximization SPECT reconstruction software," *Journal of nuclear medicine technology,* vol. 37, no. 3, pp. 179-187, 2009.

15- B. F. Hutton and Y. H. Lau, "Application of distance-dependent resolution compensation and post-reconstruction filtering for myocardial SPECT," *Physics in medicine and biology,* vol. 43, no. 6, p. 1679, 1998.

16- W. Xia, R. Lewitt, and P. Edholm, "Fourier correction for spatially variant collimator blurring in non-circular orbit SPECT," in *Nuclear Science Symposium and Medical Imaging Conference, 1992., Conference Record of the 1992 IEEE*, 1992, pp. 1026-1028: IEEE.

17- H. Onishi, N. Matsutomo, Y. Kai, Y. Kangai, H. Amijima, and T. Yamaguchi, "Evaluation of a novel normal database with matched SPECT systems and optimal pre-filter parameters for 3D-SSP," *Annals of nuclear medicine,* vol. 26, no. 1, pp. 16-25, 2012.

18- V. Moji *et al.*, "Performance evaluation of a newly developed high-resolution, dual-head animal SPECT system based on the NEMA NU1–2007 standard," *Journal of applied clinical medical physics,* vol. 15, no. 6, pp. 267-278, 2014.

19- Q. Bao, D. Newport, M. Chen, D. B. Stout, and A. F. Chatziioannou, "Performance evaluation of the inveon dedicated PET preclinical tomograph based on the NEMA NU-4 standards," *Journal of Nuclear Medicine,* vol. 50, no. 3, pp. 401-408, 2009.

20- I. Szanda *et al.*, "National Electrical Manufacturers Association NU-4 performance evaluation of the PET component of the NanoPET/CT preclinical PET/CT scanner," *Journal of nuclear medicine,* vol. 52, no. 11, pp. 1741-1747, 2011.

21- Q. Wei *et al.*, "Performance evaluation of a compact PET/SPECT/CT tri-modality system for small animal imaging applications," *Nuclear Instruments and Methods in Physics Research Section A: Accelerators, Spectrometers, Detectors and Associated Equipment,* vol. 786, pp. 147-154, 2015.

22- A. A. Harteveld *et al.*, "Using the NEMA NU 4 PET image quality phantom in multipinhole small-animal SPECT," *Journal of nuclear medicine,* vol. 52, no. 10, p. 1646, 2011.

23- H. Zaidi and W. D. Erwin, "Quantitative analysis in nuclear medicine imaging," ed: Soc Nuclear Med, 2007.

24- A. Pashazadeh *et al.*, "Experimental evaluation of the performance of HiReSPECT scanner: A high-resolution SPECT system for small animal imaging," *Frontiers in Biomedical Technologies,* vol. 1, no. 3, 2015.

25- T. R. Miller and K. S. Sampathkumaran, "Design and application of finite impulse response digital filters," *European journal of nuclear medicine,* vol. 7, no. 1, pp. 22-27, 1982.

26- I. G. Zubal and G. Wisniewski, "Understanding Fourier space and filter selection," *Journal of Nuclear Cardiology,* vol. 4, no. 3, pp. 234-243, 1997.

27- T. Iinuma and T. Nagai, "Image restoration in radioisotopic imaging systems," *Physics in Medicine & Biology,* vol. 12, no. 4, p. 501, 1967.

